RSC Advances

ROYAL SOCIETY OF CHEMISTRY

www.rsc.org/advances

RSC Advances

ARTICLE

Three-dimensional Embroidered Current Collectors for Ultra-Thick Electrodes in Batteries

Received 00th March 20xx,
Accepted 00th January 20xx

DOI: 10.1039/x0xx00000x

www.rsc.org/

N. Aguiló-Aguayo, P. Pena Espiñeira, A. P. Manian and T. Bechtold

A major bottleneck in batteries arises from the limitations in charge transfer between the active mass and the current collector. A number of strategies to increase surface of current collectors have been proposed, examples are foam electrodes, porous nano-structured surfaces, coatings with carbon nanotubes. A simple and cost efficient approach to increase surface of current collectors, which utilizes three-dimensional embroidered metal structures, is presented in this paper. In particular, for ultra-thick electrodes benefits with regard to mass loading and impedance could improve overall performance. In this paper we compare the electrochemical performance of thick $LiFePO_4$ cathodes prepared with 3D embroidered aluminium current collectors verus aluminium planar foils, over a range of mass loadings. The 3D cathodes exhibit lower impedances, higher specific capacities, and higher energy efficiencies (up to 8% gain) as compared to the planar cathodes. The 3D cathodes also exhibit greater mechanical stability. These results, which demonstrate the potential for the use of 3D embroidered current collectors in preparation of high-energy batteries, can also be extended to other chemistries.

A Introduction

Applications such as electric cars, space vehicles and portable devices (wearable and flexible electronics or implantable medical devices) require high-safety, high-energy and high-power batteries. There is generally a trade-off between power and energy densities in Li-ion batteries fabricated with planar current collectors. In order to obtain high energy densities, large amounts of electrode material are required, which causes problems in the mechanical stability (cracks appear and delamination occur), and exerts limitations on Li ion diffusion and/or on electronic conductivity, which limits the power. For this reason, it is difficult to fabricate cells that exhibit high-power and high-energy densities at the same time. High-power cells are constructed with thick current collectors to support higher currents and to better dissipate heat. For a given cell dimension, this implies a proportional decrease in amount of electrode material and thus a lower energy density. Likewise, high-energy cells require large amount of electrode material (larger capacities), and thus a proportional decrease in current collector thickness and lower current density[1,2].

Currently there are mainly three different approaches to overcome this situation: (1) the research of new chemistries to find electrode materials with higher theoretical capacities, (2) the use of porous structures or nanostructured materials to increase the amount of electrode material and contact area with the current collector, and (3) treatments to increase the mechanical stability of high amounts of electrode material.

Regarding new chemistries, lithium-rich layered oxide cathodes, lithium-sulphur or lithium-air batteries are promising candidates for high energy density batteries, which show theoretical capacities of ~240 mAh g^{-1}, ~1600 mAh g^{-1} or ~3800 mAh g^{-1}, respectively. However, before commercialization, there remain challenges to be resolved, such as in cycle performance, with voltage depression, safety issues (high reactivity of lithium metal) and low efficiencies[3–5]. Although drawbacks on the electrochemical performance, Singh et al.[6] were able to prepare thick electrodes of 70 µm and 320 µm using lithium manganese cobalt oxide cathodes on planar current collectors.

Concerning porous structures, the use of metal foams as current collectors to prepare thick electrodes are being investigated[7,8]. However, it is difficult to achieve control over some morphological aspects, such as the spatial distribution of the electrode material inside the porous structure and the uniformity in the degree of porosity. The use of polyester textiles for preparing thick electrodes (mass loadings of 140-170 mg cm^{-2}) has been reported[9]. However, as the polymer is non-conductive, a conductive coating is required to be applied on the polyester (for example, single wall carbon nanotubes). Chen et al.[10] presented flexible systems of high areal capacity using a three-dimensional hydrogel system based on carbon

Research Institute for Textile Chemistry and Textile Physics, Leopold-Franzens-Universität Innsbruck, Hoechsterstrasse 73, 6850 Dornbirn, Austria

nanotubes. The use of materials only available at a lab-scale may not be practicable for large-scale production.

In general, thick electrodes should ideally be sufficiently flexible and exhibit good adhesion between the electrode material and the current collectors. Options to improve the mechanical stability of electrodes include increasing the amount of binder in the electrode material, decreasing the particle size to improve cohesion among particles and fracture resistance[11,12]. But increasing the binder content reduces the amount of active material, negatively influences the electrolyte penetration, and can thereby limit the capacity of the batteries. The additional treatments required to reduce particle size, such as ball milling or sintering at high temperatures, can raise production costs and may also be difficult to be incorporated in commercial technological processes.

We present a strategy to prepare high energy and high power batteries using 3D embroidered current collectors from metal wires. The embroidery allows the fabrication of highly conductive 3D flexible structures with customized sizes, layouts and materials[13]. Embroidered current collectors can easily be incorporated with current battery manufacturing processes and also be used with different chemistries. Previously, we reported on the morphological characterization of embroidered electrodes[14]. In this paper, we focus on the electrochemical behaviour (galvanostatic charge/discharge cycles, EIS measurements) of thick $LiFePO_4$ cathodes prepared with 3D embroidered aluminium current collectors and compared them with the conventional aluminium foil configuration.

B Experimental

The cathode material was prepared with 88 wt.% of LiFePO4 (LFP) powders (MTI Corporation, USA), 9 wt.% of carbon black (Super C65, Timcal Belgium N. V.) and 3 wt.% styrene-butadiene rubber (SBR) binder (MTI Corporation, USA). Many studies on Li-ion batteries employ non-aqueous systems with polyvinylidene fluoride (PVdF) as binder and it shows good performance. But there are also problems with formation of harmful products such as LiF and hence currently, aqueous-based systems are increasingly being studied as they are less expensive, less toxic and more eco-friendly[15]. The use of SBR as water-soluble binder in LiFePO4 cathode material as a substitute of PVdF binder has already been reported in the literature[16–18]. The recipe used in this work is based on descriptions in the literature[19]. In future work, the recipes for the cathode will be further optimized.

The cathode slurry was cast on the current collectors, dried in an oven at 80°C overnight and then compressed at 10.2 MPa for several minutes. The Al foil used for the planar cathodes was purchased by Sigma-Aldrich®.

The embroidered current collectors were provided by V-Trion GmbH, Lustenau, Austria.

The areal density was (12.6 ± 1.0) mg cm^{-2}.

The batteries were assembled in an argon glove box using Li foil as anode and reference electrode. Celgard® 2400 (samples courtesy of Celgard, LLC) was used as a separator and 1 M $LiPF_6$ in 1:1 v/v ethylene carbonate and diethyl carbonate (EC/DEC) as electrolyte (prepared with reagents purchased from Sigma-Aldrich®).

The total thicknesses of the cathodes were measured on a thickness gauge (Karl Schröder KG Weinheim, Germany) under a normal pressure of 17.5 g cm^{-2}.

The galvanostatic charge and discharge cycles were measured on a VSP Bio-Logic system with a EC-Lab software. The EIS measurements (using AC potential with amplitude of 5 mV and frequency from 1 Hz to 1 MHz) were performed at open circuit potential (OCV) after one galvanostatic full charge and discharge cycle with 1 mA (0.07C-rate). The fitting method used was a combination of a randomized followed by Levenberg-Marquardt algorithm with 5000 iterations.

C Results and discussion

In Fig. 1 are shown pictures of the thick cathodes prepared from the 3D embroidered current collectors (without and with the cathode material) and the 2D planar current collector with a comparable mass loading. The 3D embroidered current collector is composed of 4 layers of Al wires (80 µm in diameter) embroidered with polyester back yarn on a background of polyester fabric. The four layers were embroidered in alternating layers along mutually perpendicular directions to form a pattern of squares, each with a side length of 0.625 mm. It should be noted that a variety of embroidered designs (pattern, number of layers, wire diameters, materials) are possible. One example is to create anisotropic embroidered patterns with greater numbers of Al wires at localized areas in electrodes to mitigate the heat build-up observed in conventional pouch cells[20]. Our choice of an isotropic embroidery pattern was for an easy understanding of the electrochemical behaviour. The geometric parameters of both cathodes are listed in Table 1. The surface area and volume of aluminium in the embroidered cathode were calculated considering a total of 64 Al wires in the design, each of 2 cm length and 40 µm radius. The volume of the planar cathode was computed from the aluminium thickness provided by the supplier, of 17.8 µm.

Table 1. Geometric characteristics of the 2D and 3D cathodes.

	Cathode area / mm^2	Surface area of aluminium / mm^2	Volume of aluminium/ mm^3	Surface-to-volume ratio of aluminium / mm^{-1}
2D	400	400	7.1	56
3D	400	321	6.4	50

RSC Advances

ARTICLE

The mass loadings on planar $LiFePO_4$ cathodes commonly reported are about 10 mg cm^{-2} with corresponding thicknesses of about 90 µm[21]. With greater thicknesses, there are significant problems with cracking and delamination. Here we investigated mass loadings between ca. 20-180 mg cm^{-2}. The lower end of the range was dictated by the minimum amount necessary to cover the 3D embroidered current collector of this particular layout. Beyond the upper end of the range, it was very difficult to obtain measurement-worthy planar cathodes. In the experimental range of mass loadings, it was possible to obtain workable planar electrodes, although there were problems of poor adhesion between the cathode material and the Al foil, and one in four prepared cathodes were damaged during handling. Such problems were not observed with the embroidered cathodes, as the four-layered structure provided higher mechanical stability.

The cathode thicknesses (including that of current collectors) increased linearly with mass loading as shown in Fig. 2(a). A schematic drawing of the cathodes is shown in Fig. 2(b). Linear regressions (R^2 = 0.95-0.96) yielded the same slope for both cathodes, but different intercepts. The slopes correspond to the inverse of the apparent density of the cathode material, under the assumption that it is uniformly distributed through the length, width and thickness. The apparent density (ρ) in both cathodes was found to be (1.19 ± 0.03) g cm^{-3}. The intercepts should correspond to the thickness of the solid current collector. The intercept of (17 ± 3) µm for the 2D cathode matches the thickness of the Al foil as reported by the supplier. In case of the 3D cathode, the intercept of (211 ± 17) µm corresponds to a volumetric density in the current collector of (0.59 ± 0.10) g cm^{-3}, given an areal density of 12.6 mg cm^{-2}, which is significantly different from the densities of the constituent materials (polyester, 1.38 g cm^{-3}; and aluminium, 2.70 g cm^{-3}). The discrepancy may be attributed to areas in the embroidered structure that were not accessed by the cathode material. There was no evidence of significant voids in the micro-tomography images of the embroidered cathodes[14], hence it is likely that the inaccessible parts correspond to the spaces between fibres in the polyester background and the back yarns.

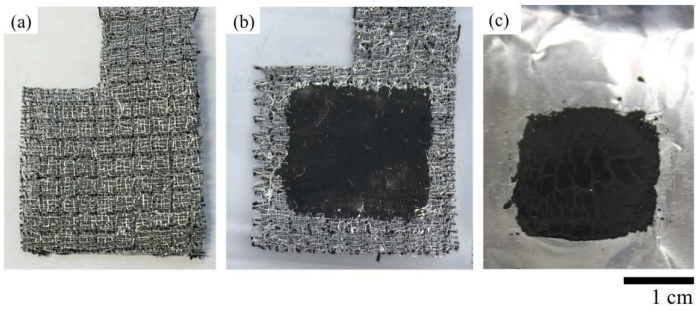

Fig. 1. Pictures of a 3D embroidered current collector (a) without and (b) with cathode material, and (c) a 2D planar current collector with cathode material of comparable mass loading. The cathode area is 2 x 2 cm^2 on both current collectors.

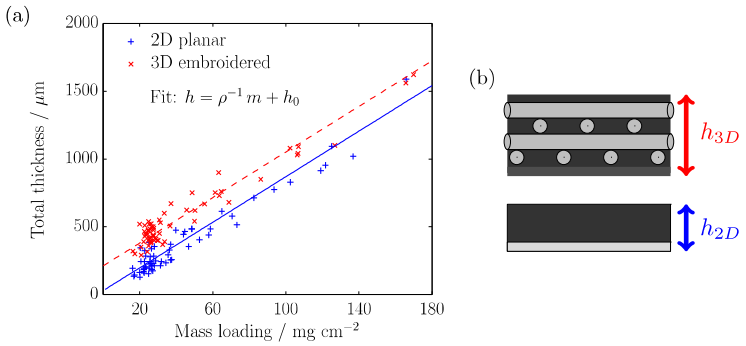

Fig. 2 (a) The total thickness, *h*, of the 2D planar and 3D embroidered cathodes as function of mass loading, *m*; and, (b) schematic illustration of the 3D and 2D cathodes.

RSC Advances

ARTICLE

The unload specific capacities from galvanostatic charge/discharge cycles performed on both cathode types are plotted as function of mass loading in Fig. 3. At 1 mA (0.25 mA cm^{-2}), there were no significant differences in performance between the 3D and planar cathodes. At higher currents, there was a decrease in unload capacity with increase in mass loading, but there were performance differences between the cathode types. Whereas the planar cathodes showed rapid losses of capacity at both 5 and 10 mA, the capacity losses in the embroidered cathodes were more gradual, and the unload capacities were even the same between 20 to 60 mg cm^{-2} at 5 mA. The capacity fade in planar $LiFePO_4$ cathodes with rising electrode thickness (mass loadings) has been attributed to ohmic resistance of the electrode material and the difficulty of electrolyte penetration through the thickness of the electrode material[22].

The lower rates in capacity fades with embroidered cathodes are indicative of a higher electronic conductivity due to the shorter electron paths to the current collectors. The embroidered cathodes were generally ~200 µm thicker in comparison to the planar cathodes, but this seems not to have negatively affected either the electrolyte penetration or the diffusion/migration of ions. It is to be expected that an increase in mass loading will lead to a progressive accumulation of cathode material above the top layer in the embroidered structures. With the four-layered embroidered cathodes used in this work, this became visually evident at mass loadings greater than ca. 75 mg cm^{-2}. This can be remedied by adding more layers to the embroidered structure.

The voltage profiles from galvanostatic charge/discharge cycles for a fixed mass loading of ca. 25 mg cm^{-2} at different currents (from 0.07 to 0.7C-rates) are shown in Fig. 4. At very low currents (1 mA), specific capacities of 140 mAh g^{-1} and potential plateaus of ~3.5 V (charge) and ~3.3 V (discharge) were obtained with both cathodes, which is in agreement with similar performances between both cathode types as observed in Fig. 3. When the current was increased from 1 to 5 mA (i.e. from 0.07 to 0.33C-rate), the embroidered cathodes showed no increase in the voltage plateaus, whereas the planar cathodes started to exhibit greater overpotentials. In addition, as the C-rate increased, there was a transition in the voltage profiles of the planar cathodes, from plateaus to gradually sloping profiles. This is attributed to rising resistance and excess heat generation due to side reactions[23,24]. These appeared to be lower for the embroidered cathodes. Measurements at C-rates higher than 0.8C were difficult as the voltages approached 4.5 V, which is the limit beyond which the EC/DEC electrolyte starts to decompose[25]. It is possible that changing the embroidery layout in 3D cathodes will further improve the electronic conductivity and allow for charge/discharge cycles at higher C-rates. The specific capacities of the embroidered electrodes may be compared with values from the literature. For example, metal foam electrodes[8] show a capacity of about 130 mAh g^{-1} at 0.6C-rate, with a thickness of about 430 µm (mass loadings of 46.5 mg cm^{-2}). In comparison, the embroidered electrodes show a capacity of about 95 mAh g^{-1} for the same thickness. The lower capacity of the embroidered electrodes is attributed to its lower electrode density (1.19 g cm^{-3}) as compared to the metal foam (1.35 g cm^{-3}). The embroidered electrode density may be improved by modifying the cathode slurry recipe, for example by introducing thickeners as sodium carboxymethyl cellulose[16,17,15] in order to avoid micro-voids on the cathode slurry as observed in previous work[14]. Further investigations will be carried out in future work.

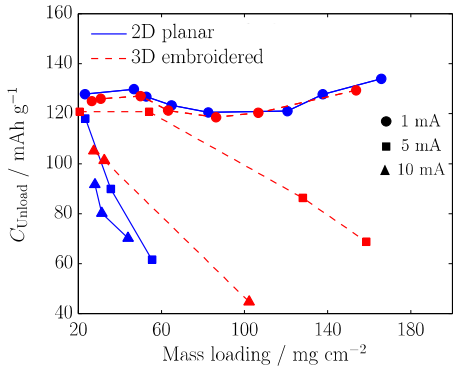

Fig. 3. Unload specific capacities as function of mass loading for 2D planar and 3D embroidered cathodes at currents of 1, 5 and 10 mA (0.25, 1.25 and 2.5 mA cm^{-2}).

The energy efficiencies for the 2D planar and 3D embroidered cathodes were calculated with Eq. 1 and are plotted as function of the applied current in Fig. 5.

$$\epsilon = \frac{\int_0^{t_d} V_d I_d dt}{\int_0^{t_c} V_c I_c dt} \qquad [1]$$

Normally the energy efficiencies of Li-ion batteries are expected to drop with rising C-rate[26], but for the 3D embroidered cathodes there was a gain of up to 8% in comparison to the planar cathodes. This is attributed to the lower internal resistance in the 3D embroidered cathodes.

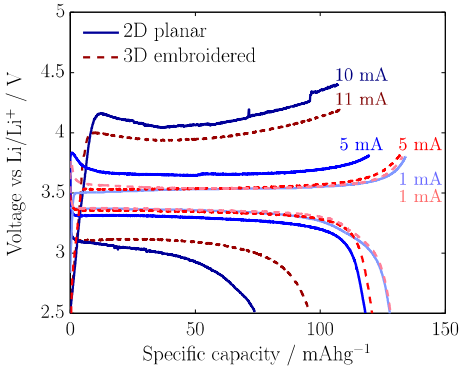

Fig. 4. Galvanostatic charge and discharge cycles for 2D planar cathodes (at 1, 5, and 10 mA) and 3D embroidered cathodes (at 1, 5 and 11 mA), at a fix mass loading of ca. 25 mg cm^{-2}.

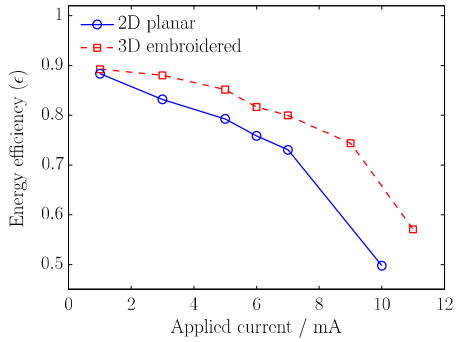

Fig. 5. Energy efficiency as function of the applied current (0.07-0.7C-rates) for the 2D planar and 3D embroidered cathodes.

There is a direct correlation between the internal resistance and battery performance. By lowering the internal resistance, higher energy efficiencies, lower heat generation and higher power performances can be achieved[27].

The results of EIS measurements conducted on cathodes with mass loadings of ca. 50 mg cm^{-2} are shown in Fig. 6. The equivalent circuit shown in the same figure, with mixed kinetics and charge-transfer control (modified Randles circuit), was fitted to the data using the Z-fit function in Bio-Logics EC-Lab software. The electrical elements included in the equivalent circuit were: electrolyte resistance, R_s; charge-transfer resistance, R_{ct}; a constant phase element (CPE), Q_{dl}, which replaces the double-layer capacitance; and a Warburg impedance term, W, which is related to the diffusion of Li ions. The results of the impedance analysis are shown in Table 2. A χ^2 value of ca. 3.5 was obtained for both fittings. The model fitting was poor at lower frequencies, likely because mass transport effects were neglected. Other models reported in the literature[28,29] were also attempted, but the goodness-of-fit were not better. The selection of the modified Randles circuit was dictated by its simplicity and ease of comprehension.

It is interesting to note that although the thicknesses of the 2D planar and 3D embroidered cathodes were different (437 µm and 630 µm, respectively), a similar semicircle depression was observed and equivalent Q_{dl} values were obtained. Both are related to the electrode porosity and roughness[30].

The R_s values (real axis intercept at high frequencies) were also comparable, and the small differences arise from the amounts of electrolyte used in the battery preparation. The R_{ct} values, which are related to the energy-barrier associated with electron transfer at electrode surfaces and the transport of redox species'[31], were almost two times larger for the 2D planar cathodes. As the aluminium surface area is similar in both cathodes (see Table 1), the lower R_{ct} values for embroidered cathodes are attributed to higher accessibility of the cathode material, translating into a higher electronic conductivity in the cathodes. This is in agreement with results from the charge/discharge cycles. For the planar cathodes, a longer tail was observed at lower frequencies and the Warburg element was 5 times higher than that for the embroidered cathodes. The differences in current collector geometry (planar foil versus wires) are likely to influence Li-ion diffusion and hence the R_{ct} and W values. All these results are in agreement with the higher electrochemical performance of the embroidered cathodes.

A further important aspect to be considered is the stability of the batteries over large numbers of cycles. The electrodes studied in this work have a minimum mass loading of about 25 mg cm^{-2}. To study stability over 100 cycles, it would require 3400 h at current density of 0.25 mA cm^{-2} (1 mA) and 680 h at current density of 1.25 mA cm^{-2} (5 mA). For higher current densities, electrolyte stability cannot be ensured due to overpotentials as shown in Fig. 4. Work is continuing on optimization of the system to be able to apply higher current densities and the stability will be studied at this time.

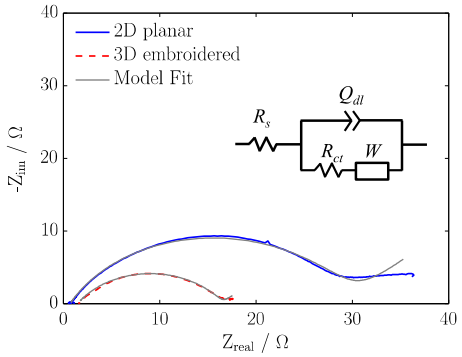

Fig. 6. Nyquist plot of impedance values for the 2D planar and 3D embroidered cathodes with mass loading of ca. 50 mg cm^{-2}. The data was fit to the equivalent circuit shown in the figure.

Table 2. Parameter estimates from the impedance analyses in Fig. 6.

	R_s / Ω	R_{ct} / Ω	Q_{dl} / µF s$^{(a-1)}$	W / Ω s$^{-0.5}$
2D	0.70	29.1	98.2 a = 0.701	14.6
3D	1.49	15.1	93.2 a = 0.639	2.64

Conclusions

The volumetric energy densities in this study were greater in the planar compared to the embroidered electrodes. But it should be noted that the mass loadings used in this work for planar electrodes are already too high. In this work, we used mass loadings from 20 to 180 mg cm^{-2} while normally the mass loadings are in the range of 5-10 mg cm^{-2} [21]. Workable planar electrodes were obtained only with great difficulty (it helped that the surface areas were small, 4 cm^2).

In contrast, with embroidered electrodes, high mass loadings are not a problem because the 3D structure acts to reinforce the cathode material and improves mechanical stability. It should also be noted that the mass loading could be further increased, without compromising performance, by increasing the number of Al layers. These are significant advantages of the embroidered structures over the planar current collectors.

In summary, it was demonstrated that thick cathodes prepared with 3D embroidered current collectors is a promising alternative for high-energy batteries. Comparisons of electrochemical performances (charge/discharge cycles and EIS measurements) highlight the following advantages of 3D embroidered cathodes in comparison to 2D planar cathodes.

(a) The 3D structure acts to reinforce the cathode material and improves mechanical stability in thick electrodes.

(b) The 3D cathodes exhibit lower charge-transfer resistances and lower Warburg impedances, which imply higher electronic conductivity.

(c) The 3D cathodes exhibit higher energy efficiencies and higher power performances. Also the level of heat generation appeared to be lower as more constant voltage profiles were obtained during charge and discharge cycles.

It should be noted that the embroidered current collectors are different from metal meshes. The embroidery technique allows for the manufacture of near-net-shapes that avoids open wire endings and thus, eliminates the risk of electrical short circuits, which are a common failure in metal meshes.

The embroidery technology makes available many options in the design of high-energy density batteries, such as (1) increasing the number of layers (higher thicknesses), (2) increasing the number density of aluminium wires per layer, and (3) increasing the lengths and widths of the current collector. The greater mechanical stability of the 3D cathodes affords the opportunity for development of flexible batteries.

Acknowledgements

Authors thank the Smart Embroidered Group for providing the 3D embroidered current collectors and Austria Forschungsförderungsgesellschaft (FFG) for funding a Research Studio Austria – RS-STE, Project No. 832002. Authors thank Thomas Froeis for management assistance. The work was supported by the project AlpStore (Alpine Space Programme 2007-2013 as part of the "European Territorial Cooperation") and the Vorarlberger Landesregierung (Europäischer Fonds für Regionale Entwicklung, EFRE, project, RS-STE).

Notes and references

1 D. Klotz, *Characterization and Modeling of Electrochemical Energy Conversion Systems by Impedance Techniques*, KIT Scientific Publishing, Karlsruhe, 2012.

2 H. Zheng, J. Li, X. Song, G. Liu and V. S. Battaglia, *Electrochim. Acta*, 2012, **71**, 258–265.

3 J. S. Lee, S. T. Kim, R. Cao, N. S. Choi, M. Liu, K. T. Lee and J. Cho, *Adv. Energy Mater.*, 2011, **1**, 34–50.

4 M. Sathiya, A. M. Abakumov, D. Foix, G. Rousse, K. Ramesha, M. Saubanère, M. L. Doublet, H. Vezin, C. P. Laisa, a S. Prakash, D. Gonbeau, G. VanTendeloo and J.-M. Tarascon, *Nat. Mater.*, 2014, **1**, 1–9.

5 D. Lv, J. Zheng, Q. Li, X. Xie, S. Ferrara, Z. Nie, L. B. Mehdi, N. D. Browning, J.-G. Zhang, G. L. Graff, J. Liu and J. Xiao, *Adv. Energy Mater.*, 2015, **5**, 1–8.

6 M. Singh, J. Kaiser and H. Hahn, *J. Electrochem. Soc.*, 2015, **162**, A1196–A1201.

7 J. Wang, P. Liu, J. Hicks-Garner, E. Sherman, S. Soukiazian, M. Verbrugge, H. Tataria, J. Musser and P. Finamore, *J. Power Sources*, 2011, **196**, 3942–3948.

8 G.-F. Yang, K.-Y. Song and S.-K. Joo, *RSC Adv.*, 2015, **5**, 16702–16706.

9 L. Hu, F. La Mantia, H. Wu, X. Xie, J. McDonough, M. Pasta and Y. Cui, *Adv. Energy Mater.*, 2011, **1**, 1012–1017.

10 Z. Chen, J. W. F. To, C. Wang, Z. Lu, N. Liu, A. Chortos, L. Pan, F. Wei, Y. Cui and Z. Bao, *Adv. Energy Mater.*, 2014, **201400207**, 1–10.

11 S. G. Santee, B. Ravdel, M. K. Gulbinska, J. S. Gnanaraj and J. F. DiCarlo, in *Lithium-ion Battery Materials and Engineering*, ed. M. K. Gulbinska, Springer, London, 1st edn., 2014, pp. 63–88.

12 G. J. Moore, F. J. Puglia and M. K. Gulbinska, in *Lithium-ion Battery Materials and Engineering*, ed. M. K. Gulbinska, Springer, London, 1st edn., 2014, pp. 89–113.

13 WO2014028958 A1, 2014.

14 N. Aguiló-Aguayo, P. Amann, P. Pena Espiñeira, J. Petrasch and T. Bechtold, *J. Power Sources*, 2016, **306**, 826–831.

15 S. Chou, Y. Pan, J. Wang, H. Liu and S. Dou, *Phys. Chem. Chem. Phys.*, 2014, **16**, 20347–20359.

16 A. Guerfi, M. Kaneko, M. Petitclerc, M. Mori and K. Zaghib, *J. Power Sources*, 2007, **163**, 1047–1052.

17 C. C. Li and Y. S. Lin, *J. Power Sources*, 2012, **220**, 413–421.

18 H. S. Kim and E. J. Shin, *Bull. Korean Chem. Soc.*, 2013, **34**, 851–855.

19 K. A. Kasvayee, Chalmers University of Technology, 2011.

20 A. Samba, N. Omar, H. Gualous, Y. Firouz, P. Van den Bossche, J. Van Mierlo and T. I. Boubekeur, *Electrochim. Acta*, 2014, **117**, 246–254.

21 K. Striebel, J. Shim, V. Srinivasan and J. Newman, *J. Electrochem. Soc.*, 2005, **152**, A664–A670.

22 D. Y. W. Yu, K. Donoue, T. Inoue, M. Fujimoto and S. Fujitani, *J. Electrochem. Soc.*, 2006, **153**, A835–A839.

23 D. Choi, D. Wang, V. V. Viswanathan, I. T. Bae, W. Wang, Z. Nie, J. G. Zhang, G. L. Graff, J. Liu, Z. Yang and T. Duong, *Electrochem. commun.*, 2010, **12**, 378–381.

24 J. H. Kim, S. C. Woo, M. S. Park, K. J. Kim, T. Yim, J. S. Kim

and Y. J. Kim, *J. Power Sources*, 2013, **229**, 190–197.
25 P. Arora, R. E. White and M. Doyle, *J. Electrochem. Soc.*, 1998, **145**, 3647–3667.
26 G. Ning, B. Haran and B. N. Popov, *J. Power Sources*, 2003, **117**, 160–169.
27 G. Pistoia, Ed., *Lithium-Ion Batteries*, Elsevier, Oxford, 1st edn., 2014.
28 F. La Mantia, J. Vetter and P. Novák, *Electrochim. Acta*, 2008, **53**, 4109–4121.
29 X.-Z. Yuan, C. Song, H. Wang and J. Zhang, *Electrochemical Impedance Spectroscopy in PEM Fuel Cells: Fundamentals and Applications*, Springer, London, 1st edn., 2010.
30 J. Bisquert, G. Garcia-Belmonte, P. Bueno, E. Longo and L. O. S. Bulhões, *J. Electroanal. Chem.*, 1998, **452**, 229–234.
31 M. A. Macdonald, Dalhousie University, 2014.

Graphical Abstract:

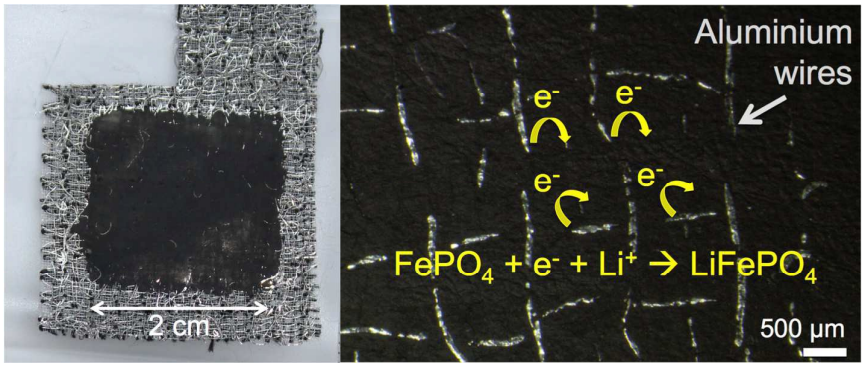

Fig. Picture (left) and photomicrograph (right) of the embroidered $LiFePO_4$ cathode. The discharge reaction on the electrode surface is also illustrated.